

Pseudospin exchange interactions in d^7 cobalt compounds: Possible realization of the Kitaev model

Huimei Liu and Giniyat Khaliullin

Max Planck Institute for Solid State Research, Heisenbergstrasse 1, D-70569 Stuttgart, Germany

(Dated: January 8, 2018)

The current efforts to find the materials hosting Kitaev model physics have been focused on Mott insulators of d^5 pseudospin-1/2 ions Ir^{4+} and Ru^{3+} with $t_{2g}^5 (S = 1/2, L = 1)$ electronic configuration. Here we propose that the Kitaev model can be realized in materials based on d^7 ions with $t_{2g}^5 e_g^2 (S = 3/2, L = 1)$ configuration such as Co^{2+} , which also host the pseudospin-1/2 magnetism. Considering possible exchange processes, we have derived the d^7 pseudospin-1/2 interactions in 90° bonding geometry. The obtained Hamiltonian comprises the bond-directional Kitaev K and isotropic Heisenberg J interactions as in the case of d^5 ions. However, we find that the presence of additional, spin-active e_g electrons radically changes the balance between Kitaev and Heisenberg couplings. Most remarkably, we show that the exchange processes involving e_g spins are highly sensitive to whether the system is in Mott ($U < \Delta$) or charge-transfer ($U > \Delta$) insulating regime. In the latter case, to which many cobalt compounds do actually belong, the antiferromagnetic Heisenberg coupling J is strongly suppressed and spin-liquid phase can be stabilized. The results suggest cobalt-based materials as promising candidates for the realization of the Kitaev model.

I. INTRODUCTION

In recent years, the Kitaev honeycomb model [1] and its various extensions have attracted much attention (see the recent reviews [2–6] and references therein). In this model, the spins-1/2 interact via a strongly anisotropic, bond-dependent Ising couplings $S_i^x S_{i+\gamma_1}^x$, $S_i^y S_{i+\gamma_2}^y$, and $S_i^z S_{i+\gamma_3}^z$, acting on three nearest-neighbor γ_1 , γ_2 , and γ_3 bonds of a tri-coordinated honeycomb lattice. A mutual orthogonality of the Ising-axis directions on different γ bonds results in strong frustration, driving the spins into a quantum disordered state.

Physically, the bond-dependent exchange couplings as in the Kitaev model may arise from an unquenched orbital contribution \mathbf{L} to the magnetic moments. Due to the non-spherical shape of the electron orbitals, the orbital moment interactions in transition-metal compounds are strongly anisotropic, both in real and angular momentum spaces [7–9]. By virtue of spin-orbit coupling (SOC), this property of orbital interactions is inherited by total angular momentum $\mathbf{J} = \mathbf{L} + \mathbf{S}$ of magnetic ions, as demonstrated by explicit calculations of magnetic Hamiltonians in the limit of strong SOC [9–12]. Apart from magnetism, SOC driven Kitaev-type interactions may lead also to exotic superconducting states in doped Mott insulators [9, 13–15].

From the materials perspective, having unquenched orbital moments \mathbf{L} in solids is not rare but requires special conditions: (i) lattice distortions caused by the steric effects are small so that there remains the orbital (quasi)degeneracy, and (ii) Jahn-Teller coupling and superexchange interactions, which favor ordering of the real orbitals and hence quench the \mathbf{L} moments, are weaker than intraionic spin-orbit coupling (SOC). Under these conditions, typical for late transition-metal (TM) compounds with t_{2g} orbital degeneracy, the exchange interactions between magnetic ions can be formulated in terms

of pseudospins \tilde{S} operating within the ground-state spin-orbit manifold. Degeneracy of this manifold, and hence the \tilde{S} value depends on electron configuration of the TM ions and local crystal field symmetry.

In the context of the Kitaev model, the TM ions that possess pseudospin-1/2 ground state doublet are of particular interest. In the past, $3d$ -cobalt compounds CoO , KCoF_3 , CoCl_2 , etc. have been canonical examples of the pseudospin-1/2 magnetism (see, e.g., Refs. 16–19), and, more recently, $4d$ and $5d$ compounds RuCl_3 , Sr_2IrO_4 , Na_2IrO_3 , etc. came into focus (see reviews [5, 6]). In cobaltates, the d^7 ions Co^{2+} in an octahedral crystal field have a predominantly $t_{2g}^5 e_g^2$ configuration with $S = 3/2$ and an effective $L = 1$ moments [20], forming a pseudospin-1/2 doublet in their ground state (see Fig. 1). This is similar to the case of d^5 ions Ru^{3+} and Ir^{4+} with $t_{2g}^5 (S = 1/2, L = 1)$ configuration, and, on symmetry grounds, the pseudospin-1/2 exchange Hamiltonians in both d^7 and d^5 systems must have the identical form. However, the presence of additional, spin-active e_g electrons in d^7 cobaltates is expected to have a strong impact on the actual values of exchange parameters. In particular, they should affect the strength of the Kitaev-type couplings relative to other terms in the Hamiltonian.

In this paper, we derive the d^7 pseudospin-1/2 interactions in the edge-shared, 90° bonding geometry, including various nearest-neighbor hopping processes allowed by symmetry. As expected, the spin-orbital exchange Hamiltonian projected onto pseudospin $\tilde{S} = 1/2$ subspace comprises the isotropic Heisenberg $\tilde{J}\tilde{\mathbf{S}}_i \cdot \tilde{\mathbf{S}}_j$ and bond-dependent Kitaev $K\tilde{S}_i^\gamma \tilde{S}_j^\gamma$ couplings, as in the case of d^5 ions [9–12]. (Non-diagonal components of the exchange tensor Γ_{xy} [21] are also present but not dominant.) We find that the presence of e_g spins in d^7 configuration has important consequences on relative values of the parameters J and K . In contrast to d^5 case, where

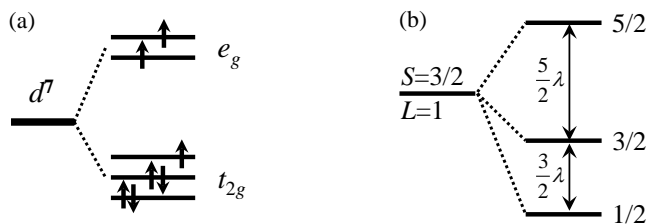


FIG. 1. (a) High-spin state of $d^7(t_{2g}^5 e_g^2)$ configuration in an octahedral crystal field. (b) Splitting of $S = 3/2, L = 1$ manifold under spin-orbit coupling $\lambda(\mathbf{LS})$, resulting in pseudospin-1/2 ground state doublet.

the leading exchange term $\propto 4t^2/U$ does not contribute to the pseudospin interactions [9], we find here that both Heisenberg J and Kitaev K couplings appear already in the leading order of $4t^2/U$ or $4t^2/\Delta$ (where U and Δ stand for intraionic Coulomb and pd charge-transfer energies, correspondingly). Most importantly, the e_g spin contribution to J is always ferromagnetic and it largely compensates antiferromagnetic contributions from t_{2g} orbitals. As a result, net value of isotropic J coupling is strongly reduced, in particular in the charge-transfer regime of $U > \Delta$ relevant to cobaltates [22]. This mechanism of suppressing the Heisenberg J term is specific to the d^7 pseudospin systems, and it suggests an alternative way to access the desired parameter regime of $K \gg J$ with spin-liquid ground state.

Our study is partially motivated by the recent experiments [23–26] on cobalt compounds $\text{Na}_2\text{Co}_2\text{TeO}_6$ and $\text{Na}_3\text{Co}_2\text{SbO}_6$ with a layered hexagonal structure. In both systems, the d^7 ions Co^{2+} form a nearly perfect honeycomb lattice and develop a zigzag-type antiferromagnetic order at low temperatures, analogous to that observed in d^5 pseudospin-1/2 materials RuCl_3 and Na_2IrO_3 . This similarity may not be accidental, and the results presented in this work suggest that d^7 cobalt compounds may indeed harbor pseudospin-1/2 Kitaev-Heisenberg model and related physics.

This paper is organized as follows. Section II introduces the single ion Hamiltonian and d^7 pseudospin-1/2 wave functions. Section III discusses various exchange processes between the d^7 TM ions in 90° bonding geometry, relevant for a honeycomb lattice cobaltates, and derives the corresponding exchange parameters as a function of material parameters. Section IV considers interplay between different exchange mechanisms and the resulting phase diagrams. The main results and conclusions are summarized in Sec. V. Appendix A discusses Hund’s coupling corrections to the exchange parameters.

II. SINGLE ION LEVELS AND WAVE FUNCTIONS

The high-spin $S = 3/2$ Co^{2+} ion in the octahedral field has a predominantly $t_{2g}^5 e_g^2$ electronic configuration shown in Fig. 1(a). (We neglect the admixture of $t_{2g}^4 e_g^3$ state, since its spectral weight is ~ 0.06 only [18, 27].) The threefold orbital degeneracy of this configuration can conveniently be described in terms of an effective angular momentum $L = 1$ [20]. Further, the spin and orbital moments are coupled via spin-orbit coupling $\lambda(\mathbf{LS})$, with $\lambda > 0$. This results in a level structure shown in Fig. 1(b), with the ground-state Kramers doublet hosting a pseudospin 1/2. The actual value of λ is material dependent due to various factors such as covalency effects, and can experimentally be quantified from excitation energy $\frac{3}{2}\lambda$ between spin-orbit levels $1/2 \rightarrow 3/2$ in Fig. 1(b). In Co^{2+} perovskite KCoF_3 , this transition (termed as “spin-orbit exciton”) was observed at ~ 40 meV by the inelastic neutron scattering [16, 17].

In the cubic crystal field, Co^{2+} pseudospin-1/2 wavefunctions $|\pm \frac{1}{2}\rangle$ read, in the basis of $|S_z, L_z\rangle$ states, as follows:

$$\begin{aligned} \left|+\frac{1}{2}\right\rangle &= \frac{1}{\sqrt{2}}\left|\frac{3}{2}, -1\right\rangle - \frac{1}{\sqrt{3}}\left|\frac{1}{2}, 0\right\rangle + \frac{1}{\sqrt{6}}\left|-\frac{1}{2}, 1\right\rangle, \\ \left|-\frac{1}{2}\right\rangle &= \frac{1}{\sqrt{2}}\left|-\frac{3}{2}, 1\right\rangle - \frac{1}{\sqrt{3}}\left|-\frac{1}{2}, 0\right\rangle + \frac{1}{\sqrt{6}}\left|\frac{1}{2}, -1\right\rangle. \end{aligned} \quad (1)$$

As in case of d^5 systems [9], we derive the d^7 pseudospin-1/2 Hamiltonian in the following way: (i) calculate first the exchange interactions that operate in full spin-orbital Hilbert space, and (ii) project them onto low-energy pseudospin $\tilde{S} = 1/2$ sector defined now by the wave functions (1). The resulting Hamiltonian does not include the transitions to high-energy states with total angular momentum $3/2$ and $5/2$ [Fig. 1(b)]; the corresponding spin-orbit excitations are assumed to have only perturbative effects on magnetic order and fluctuations. This approximation, and hence a notion of “pseudospin” itself, is physically justified if the pseudospin interactions are weaker than spin-orbit coupling. In practice, this criteria implies that the spin-orbit exciton modes are separated from low-energy pseudospin-1/2 magnons, as indeed observed in cobaltates KCoF_3 [16, 17], GeCo_2O_4 [28], $\text{NaCaCo}_2\text{F}_7$ [29], or in iridate Sr_2IrO_4 [30, 31].

The calculations below are based on perturbation theory assuming that the hopping parameters are smaller than excitation energies of the intermediate states created during the hopping processes. Specifically, this implies a hopping amplitude t_{pd} between oxygen p and TM-ion d states is smaller than charge-transfer gap Δ , and hopping t between TM d orbitals is much smaller than Coulomb U as well as charge-transfer gap Δ , such that exchange parameters $\propto 4t^2/U$ or $\propto 4t^2/\Delta$ resulting from calculations are much less than U and Δ values. Put

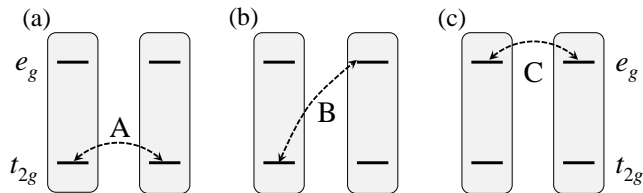


FIG. 2. Three different classes of the exchange processes, A, B, and C, derived from interactions between (a) t_{2g} and t_{2g} , (b) t_{2g} and e_g , and (c) e_g and e_g spin-orbital levels. In the text, the corresponding contributions to the exchange Hamiltonian are denoted as \mathcal{H}_A , \mathcal{H}_B , and \mathcal{H}_C .

differently, it is assumed that system is a good insulator where the magnetic and charge energy scales are well separated, which is indeed the case in many cobalt compounds with magnon energies well below 100 meV (see, e.g., Refs. [16, 17, 28, 29]).

III. EXCHANGE PROCESSES AND INTERACTIONS

Since the spins residing on e_g orbitals also play an active role in the exchange processes, the spin-orbital model for d^7 ions is far more complex than in d^5 systems with t_{2g} only orbitals. To make the structure of the paper more transparent, we divide the exchange processes into three classes (see Fig. 2): exchange between (A) t_{2g} and t_{2g} orbitals, (B) t_{2g} and e_g orbitals, and (C) e_g and e_g orbitals.

Accordingly, this section is divided into three parts, subsections A, B, and C, where the above exchange contributions A(t_{2g} - t_{2g}), B(t_{2g} - e_g), and C(e_g - e_g) are considered. The subsections are further structured according to three physically distinct exchange mechanisms: (i) the U processes, (ii) the charge-transfer processes, and (iii) the cyclic-exchange processes. The U processes involve virtual excitations with energies of the order of Hubbard U and they are dominant in Mott-Hubbard-type insulators with $U < \Delta$, while the latter two processes become important in charge-transfer-type insulators with $\Delta < U$, in terms of Zaanen-Sawatsky-Allen classification [22]. Although cobalt compounds typically belong to the latter category, we will show the results for arbitrary values of ratio U/Δ for the sake of generality.

A. t_{2g} - t_{2g} exchange

1. Intersite U processes

We consider virtual charge transitions of the type $d_i^7 d_j^7 \rightarrow d_i^6 d_j^8$, created by hopping of t_{2g} electrons between two nearest-neighbor magnetic ions. The excitation energy associated with this intersite charge fluctuation is

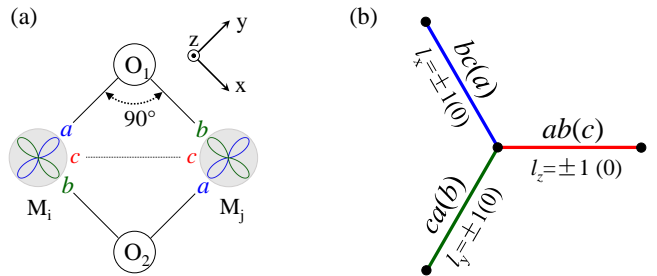


FIG. 3. (a) A 90° M-O-M bonding geometry, where magnetic ions M_i and M_j interact via two oxygen ions O_1 and O_2 . Two out of three t_{2g} orbitals, here $a = d_{yz}$ and $b = d_{zx}$, participate in the superexchange process by virtue of an indirect hopping t_{ab} via the oxygen p_z orbitals. The remaining orbital $c = d_{xy}$ (not shown) contributes to spin exchange via a direct hopping t_{cc} . (b) Three types of bonds and corresponding orbital selective hopping geometry. On the horizontal (red) bond, the $ab(c)$ should read as $t_{ab}(t_{cc})$, with $t_{ab} = t$ and $t_{cc} = -t'$. This bond will be referred to as "c bond" in the text. In terms of the t_{2g} orbital angular momentum, ab pair represents the $l_z = \pm 1$ doublet, while c orbital corresponds to the $l_z = 0$ state. The hopping geometry on two other (blue and green) bonds follows from symmetry.

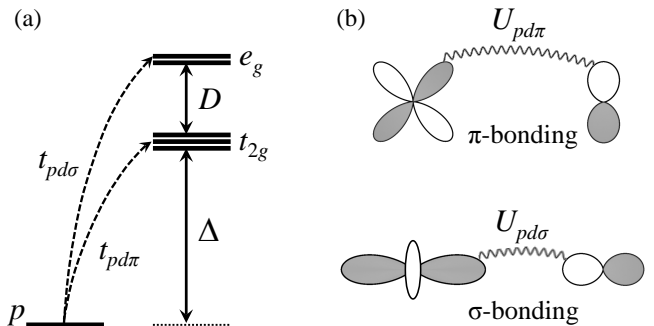


FIG. 4. (a) Schematic of oxygen p and transition-metal ion $d(t_{2g}, e_g)$ energy levels. $t_{pd\pi}$ ($t_{pd\sigma}$) is the hopping integral between p and t_{2g} (e_g) orbitals. The corresponding pd charge-transfer gaps are Δ and $\Delta + D$. (b) Two types of the pd -covalent bondings, π and σ , involving t_{2g} and e_g orbitals correspondingly. A d electron and p hole created by the pd transition experience the Coulomb attraction, which is stronger in σ -bonding channel: $U_{pd\sigma} > U_{pd\pi}$. This reduces the effective value of D from a single-electron cubic splitting $10Dq$ by $U_{pd\sigma} - U_{pd\pi} > 0$ (see text).

Coulomb repulsion U , and the resulting exchange couplings scale as t^2/U .

In a 90° bonding geometry [see Fig. 3(a)], the nearest-neighbor t_{2g} orbital hopping along the c bond can be written as [9, 13, 32, 33]:

$$\mathcal{H}_t^{(c)} = t(a_{i\sigma}^\dagger b_{j\sigma} + b_{i\sigma}^\dagger a_{j\sigma}) - t'c_{i\sigma}^\dagger c_{j\sigma} + \text{H.c.} \quad (2)$$

Here, summation over spin projection σ is implied. Parameter $t = t_{pd\pi}^2/\Delta$ is the hopping amplitude between

$a = d_{yz}$ and $b = d_{zx}$ orbitals, originating from d - p - d process via the p - d charge-transfer gap Δ [Fig. 4(a)]. $t' > 0$ is given by a direct overlap of $c = d_{xy}$ orbitals. Note that oxygen-mediated t hopping in Eq. (2) changes the orbital color. In terms of effective angular momentum $l = 1$ of t_{2g} electron, $d_{\pm 1}^\dagger = \mp(d_{yz}^\dagger \pm id_{zx}^\dagger)/\sqrt{2}$, this term reads as $it(d_{1,\sigma}^\dagger d_{-1,\sigma} - d_{-1,\sigma}^\dagger d_{1,\sigma})_{ij}$, making it clear that hopping does not conserve angular momentum of a pair and hence may lead to anisotropic exchange interactions. This is in contrast to 180° bonding geometry with orbital-conserving hopping, $t(a_{i\sigma}^\dagger a_{j\sigma} + b_{i\sigma}^\dagger b_{j\sigma}) \rightarrow t(d_{1,\sigma}^\dagger d_{1,\sigma} + d_{-1,\sigma}^\dagger d_{-1,\sigma})_{ij}$.

As shown in Fig. 5 and detailed in its caption, there are several exchange processes involving different combinations of oxygen-mediated t and direct t' hoppings. Collecting all these terms, one arrives at the following spin-orbital Hamiltonian for a pair along c bond:

$$\begin{aligned} \mathcal{H}_{A1}^{(c)} = & \frac{4t^2}{9U} (\mathbf{S}_i \cdot \mathbf{S}_j + S^2) \left[(n_{ia}n_{jb} + a_i^\dagger b_i a_j^\dagger b_j) + (a \leftrightarrow b) \right] \\ & - \frac{4tt'}{9U} (\mathbf{S}_i \cdot \mathbf{S}_j + S^2) \left[(a_i^\dagger c_i c_j^\dagger b_j + c_i^\dagger a_i b_j^\dagger c_j) + (a \leftrightarrow b) \right] \\ & + \frac{4t'^2}{9U} (\mathbf{S}_i \cdot \mathbf{S}_j - S^2) n_{ic}n_{jc}. \end{aligned} \quad (3)$$

In this expression, spin $S = 3/2$ stands for high-spin configuration of the d^7 ion. We used a relation $\mathbf{s} = \frac{1}{2S}\mathbf{S}$ between t_{2g} -hole spin \mathbf{s} (one-half) and total spin \mathbf{S} , as dictated by Hund's coupling. [In principle, the first contribution above contains also a pure density term $-(t^2/U)(2 - n_{ic} - n_{jc})$, which is irrelevant and thus not shown.]

Next, we project the exchange Hamiltonian Eq. (3) onto pseudospin $\tilde{S} = 1/2$ subspace defined by wavefunctions (1). A direct comparison of the matrix elements gives the following relations:

$$S_x = \frac{5}{3}\tilde{S}_x, \quad S_x n_a = \frac{1}{3}\tilde{S}_x, \quad S_x n_{b/c} = \frac{2}{3}\tilde{S}_x, \quad (4)$$

$$a^\dagger b = \frac{i}{3}\tilde{S}_z, \quad b^\dagger c = \frac{i}{3}\tilde{S}_x, \quad c^\dagger a = \frac{i}{3}\tilde{S}_y, \quad (5)$$

$$S_x a^\dagger b = \frac{1}{6}\tilde{S}_y, \quad S_x b^\dagger c = \frac{5i}{12}, \quad S_x c^\dagger a = \frac{1}{6}\tilde{S}_z. \quad (6)$$

The other combinations of spin and orbital operators involving S_y and S_z can be obtained from the above mappings by symmetry. As a result, we find the following pseudospin exchange Hamiltonian:

$$\begin{aligned} \mathcal{H}_{A1}^{(c)} = & \frac{2t^2}{9U} \left(\tilde{\mathbf{S}}_i \cdot \tilde{\mathbf{S}}_j - \frac{2}{9}\tilde{S}_i^z \tilde{S}_j^z \right) \\ & + \left(\frac{4}{9} \right)^2 \frac{tt'}{U} \left(\tilde{S}_i^x \tilde{S}_j^y + \tilde{S}_i^y \tilde{S}_j^x \right) \\ & + \left(\frac{4}{9} \right)^2 \frac{t'^2}{U} \left(\tilde{\mathbf{S}}_i \cdot \tilde{\mathbf{S}}_j - \frac{3}{4}\tilde{S}_i^z \tilde{S}_j^z \right), \end{aligned} \quad (7)$$

which comprises antiferromagnetic (AF) Heisenberg $\tilde{\mathbf{S}}_i \cdot \tilde{\mathbf{S}}_j$, ferromagnetic (FM) Kitaev $\tilde{S}_i^z \tilde{S}_j^z$, and non-diagonal $\tilde{S}_i^x \tilde{S}_j^y$ -type interactions. Interactions on other (a and b)

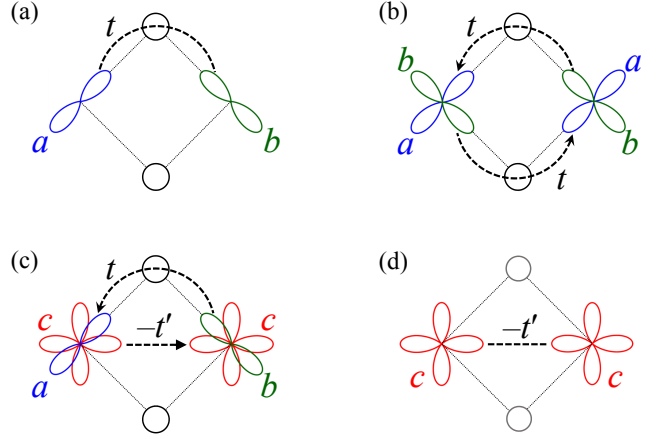


FIG. 5. Schematic of the nearest-neighbor hoppings of t_{2g} orbitals a (blue), b (green), and c (red). Oxygen p_z orbitals are depicted as open circles. (a) Orbital a to b hopping (and vice versa) through an upper oxygen p_z orbital. There is no orbital exchange during this process, and the orbital operator is $n_{ia}n_{jb}$; similar process through the lower oxygen gives $n_{ib}n_{ja}$. (b) The exchange process involving both upper and lower oxygen ions. This process changes the orbital state $b_i b_j$ into $a_i a_j$. The corresponding operator is $a_i^\dagger a_j^\dagger b_j b_i + \text{H.c.}$ (c) Cross-term involving t_{ab} hopping via oxygen and direct t' hopping of c orbital. The orbital exchange operator is $a_i^\dagger c_j^\dagger b_j c_i$, and similar process using the lower oxygen gives $b_i^\dagger c_j^\dagger a_j c_i$. (d) Direct hopping between the c orbitals.

bonds follow from symmetry (cyclic permutations among $\tilde{S}^x, \tilde{S}^y, \tilde{S}^z$). As already noticed above, the U -process interactions of the order of t^2/U do not vanish in the present case, in sharp contrast to d^5 pseudospin-1/2 systems [9]. This is due to different internal structure of pseudospin wave functions in Eq. (1), as compared to that of d^5 ions with pure t_{2g} orbitals.

2. Charge-transfer processes

We consider now virtual pd charge-transfer excitations of the type $d_i^7 - p^6 - d_j^7 \rightarrow d_i^8 - p^4 - d_j^8$, when two holes are created on an oxygen site bridging nearest-neighbor magnetic ions i and j , see Figs. 6(a) and 6(b). If the holes meet at the same p orbital, intermediate-state energy is $2\Delta + U_p$, where U_p is Coulomb repulsion on oxygen site. This contribution is antiferromagnetic, since two holes have to be in spin-singlet state. If the holes occupy different orbitals [e.g., p_z and p_y as in Fig. 6(b)], the intermediate-state energy depends on whether the two holes form triplet (T) or singlet (S) states, with $E_T = 2\Delta + U_p' - J_H^p$ and $E_S = 2\Delta + U_p' + J_H^p$, where $U_p' = U_p - 2J_H^p$, and J_H^p is Hund's coupling on oxygen that splits T and S states [see Fig. 6(c)]. The exchange

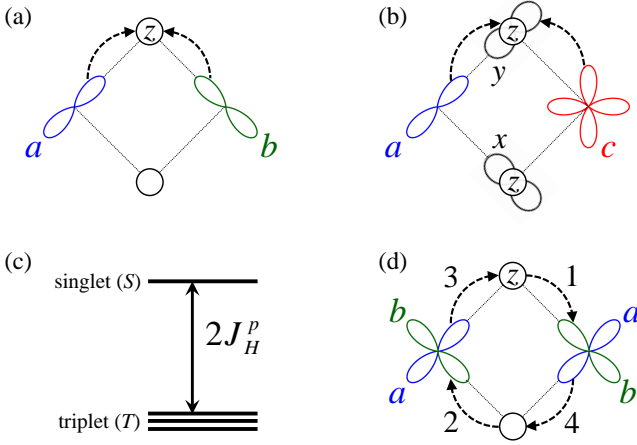


FIG. 6. (a),(b) Schematic of charge-transfer processes when two holes meet on an oxygen site. In (a), they arrive at the same p_z orbital, while in (b) two holes occupy different p orbitals ($z = p_z$ and $y = p_y$) and interact via Hund's coupling J_H^p . The latter results in (c) singlet-triplet splitting of the intermediate two-hole states of oxygen. (d) An example of the cyclic exchange process. The numbers 1, 2, 3, 4 represent the time order of the pd hoppings of electrons. During this process, the particles cycle within the plaquette avoiding a direct contact with each other. The ions interchange their spin and orbital quantum numbers, and this can be expressed as a product of Dirac spin permutation operator and orbital operator $b_i^\dagger b_j^\dagger a_j a_i$.

energy gain in this case is

$$-4t^2 \left(\frac{1}{E_T} P_T + \frac{1}{E_S} P_S \right), \quad (8)$$

where $P_T = \frac{3}{4} + (\mathbf{s}_i \cdot \mathbf{s}_j)$ and $P_S = \frac{1}{4} - (\mathbf{s}_i \cdot \mathbf{s}_j)$ are triplet- and singlet-state projectors. Since $E_T < E_S$, this contribution is of a ferromagnetic nature.

Collecting the above charge-transfer contributions, we obtain the following spin-orbital Hamiltonian for a c -bond pair:

$$\begin{aligned} \mathcal{H}_{A2}^{(c)} = & \frac{4}{9} \frac{t^2}{\Delta + \frac{U_p}{2}} (\mathbf{S}_i \cdot \mathbf{S}_j - S^2) (n_{ia} n_{jb} + n_{ib} n_{ja}) \\ & - \frac{2}{9} \frac{t^2 J_H^p}{(\Delta + \frac{U_p}{2})^2} \mathbf{S}_i \cdot \mathbf{S}_j (n_{ic} + n_{jc}). \end{aligned} \quad (9)$$

Projecting this Hamiltonian onto the ground-state doublet (1), we find:

$$\begin{aligned} \mathcal{H}_{A2}^{(c)} = & \frac{16}{81} \frac{t^2}{\Delta + \frac{U_p}{2}} (\tilde{\mathbf{S}}_i \cdot \tilde{\mathbf{S}}_j + \tilde{S}_i^z \tilde{S}_j^z) \\ & - \frac{40}{81} \frac{t^2 J_H^p}{(\Delta + \frac{U_p}{2})^2} \left(\tilde{\mathbf{S}}_i \cdot \tilde{\mathbf{S}}_j - \frac{1}{2} \tilde{S}_i^z \tilde{S}_j^z \right). \end{aligned} \quad (10)$$

It follows that charge-transfer contribution to the Kitaev term is of a positive sign (i.e., AF), while Heisenberg coupling can be either AF or FM depending on Hund's coupling strength J_H^p .

3. Cyclic exchange processes

The nearest-neighbor cyclic exchange process [see Fig. 6(d) and its caption] is special to 90° bonding geometry. This exchange involves two oxygen sites (O_1 and O_2) where two holes are generated in the intermediate state, i.e., $d_i^7 - (p_1^6, p_2^6) - d_j^7 \rightarrow d_i^8 - (p_1^5, p_2^5) - d_j^8$. This process is distinct from the above U and $2\Delta + U_p$ processes in a sense that the excited two particles do not meet either at TM or oxygen ions, and thus no direct Coulomb repulsion is encountered. Exchange interaction in this case is of a pure quantum-mechanical origin: during the cyclic motion of the electrons, two TM ions interchange their spin and orbital quantum numbers, and the resulting kinetic energy gain depends on symmetry of a wave function and hence on total spin of a pair. The cyclic exchange Hamiltonian can be expressed via Dirac spin permutation operator $(2\mathbf{s}_i \cdot \mathbf{s}_j + \frac{1}{2}) \rightarrow (\mathbf{S}_i \cdot \mathbf{S}_j + S^2)/2S^2$ and the orbital exchange operators as follows:

$$\mathcal{H}_{A3}^{(c)} = \frac{4}{9} \frac{t^2}{\Delta} (\mathbf{S}_i \cdot \mathbf{S}_j + S^2) (a_i^\dagger b_i a_j^\dagger b_j + b_i^\dagger a_i b_j^\dagger a_j). \quad (11)$$

After projecting onto a pseudospin-1/2 doublet (1), this Hamiltonian reads as follows:

$$\mathcal{H}_{A3}^{(c)} = \frac{2}{81} \frac{t^2}{\Delta} (\tilde{\mathbf{S}}_i \cdot \tilde{\mathbf{S}}_j - 10\tilde{S}_i^z \tilde{S}_j^z). \quad (12)$$

It follows from this equation that the cyclic exchange leads to nearly pure Kitaev coupling with $K = -10J$. Taken alone, this exchange mechanism would lead to the spin-liquid ground state (which is stable for $-K > 8J$ [12, 34]).

Now, we put together all three $t_{2g} - t_{2g}$ exchange contributions considered in this subsection, and obtain

$$\begin{aligned} \mathcal{H}_A^{(c)} = & \mathcal{H}_{A1}^{(c)} + \mathcal{H}_{A2}^{(c)} + \mathcal{H}_{A3}^{(c)} \\ = & J_A \tilde{\mathbf{S}}_i \cdot \tilde{\mathbf{S}}_j + K_A \tilde{S}_i^z \tilde{S}_j^z + \Gamma_A (\tilde{S}_i^x \tilde{S}_j^y + \tilde{S}_i^y \tilde{S}_j^x), \end{aligned} \quad (13)$$

with the following parameters:

$$\begin{aligned} J_A = & +\frac{2}{9} t^2 \left[\left(1 + \frac{8\kappa^2}{9}\right) \frac{1}{U} + \frac{8}{9} \frac{1}{\Delta + \frac{U_p}{2}} - \frac{20}{9} \frac{J_H^p}{(\Delta + \frac{U_p}{2})^2} + \frac{1}{9\Delta} \right], \\ K_A = & -\frac{2}{9} t^2 \left[\left(\frac{2}{9} + \frac{2\kappa^2}{3}\right) \frac{1}{U} - \frac{8}{9} \frac{1}{\Delta + \frac{U_p}{2}} - \frac{10}{9} \frac{J_H^p}{(\Delta + \frac{U_p}{2})^2} + \frac{10}{9\Delta} \right], \\ \Gamma_A = & \frac{2}{9} t^2 \frac{8\kappa}{9U}. \end{aligned} \quad (14)$$

Here, a ratio $\kappa = t'/t$ between a direct t' and oxygen-mediated t hoppings (depending on material chemistry) is introduced. Typically, $\kappa < 1$ for $3d$ -ion wave functions, which implies that non-diagonal component of the exchange tensor Γ is small.

Regarding Heisenberg J and Kitaev K couplings, it follows from Eq. (14) that their ratio strongly depends on whether the system is in Mott ($U < \Delta$) or charge-transfer ($U > \Delta$) insulating regime [22]. In the first case, the U

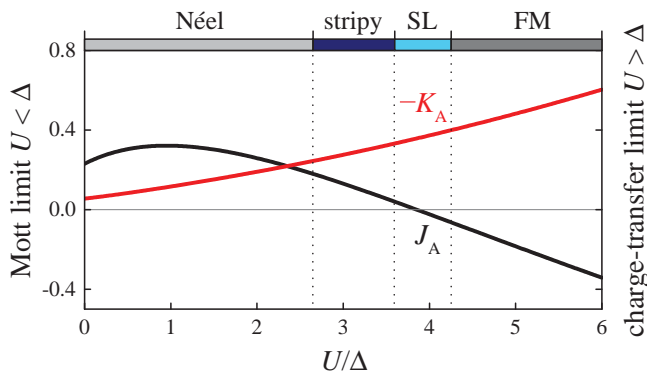


FIG. 7. t_{2g} - t_{2g} contribution to Heisenberg (J_A) and Kitaev ($-K_A$) couplings in units of t^2/U as a function of U/Δ . The parameters used are: $J_H^p/U_p=0.3$ [35], $\kappa=0.2$, and $U_p/U=0.7$. The phase boundaries are obtained using the results of Refs. 12 and 34. SL is the abbreviation for spin liquid state. In the "Mott limit" of $\Delta \gg U$, interactions are dominated by the U processes $\propto t^2/U$.

processes dominate resulting in $J_A > -K_A$. This ratio is reversed when charge-transfer and cyclic exchange processes start to dominate as U/Δ increases. Figure 7, where we plot J_A and K_A values as a function of U/Δ , clearly illustrates this trend. For $\kappa = 0.2$ used in this figure, parameter Γ_A is small, $\Gamma_A \ll (J_A, K_A)$, and not shown.

The phase diagram of the Kitaev-Heisenberg model as a function of K/J has been quantified in Refs. 12 and 34. Using the results of these works, we have indicated in Fig. 7 the phase boundaries. In the Mott insulating regime of small U/Δ (i.e., $\Delta \gg U \gg t$), Néel and stripy AF states are stable. The spin-liquid state with $-K_A \gg |J_A|$ is expected around $U/\Delta \sim 4$. In strong charge-transfer limit ($U \gg \Delta \gg t$), this state gives way to the FM phase.

B. t_{2g} - e_g exchange

In 90° bonding geometry, hopping between t_{2g} and e_g orbitals is actually the largest one, since it involves σ -type $t_{pd\sigma}$ ($\simeq 2t_{pd\pi}$) overlap. Therefore, the t_{2g} - e_g exchange contributions to J and K couplings are essential. In this subsection, we quantify these contributions. Technically, the calculations closely follow those in previous section, with only difference arising from different geometry of the orbitals involved.

1. Intersite U processes

For a c -bond pair, hopping between c and $3z^2 - r^2$ -type orbitals, shown in Fig. 8(a), is only finite [9, 36]; the other t_{2g} - e_g matrix elements vanish due to quantum

interference between pd virtual hoppings through the upper and lower oxygen ions. Since e_g states are half-filled in d^7 configuration, the exchange interaction should be antiferromagnetic, according to Goodenough-Kanamori rules [37]. Explicit calculations of the energy gain from hopping processes in Fig. 8(a) indeed result in AF spin coupling

$$\mathcal{H}_{\text{BI}}^{(c)} = \frac{4\alpha}{9} \frac{tt_e}{\tilde{U}} (\mathbf{S}_i \cdot \mathbf{S}_j - S^2)(n_{ic} + n_{jc}). \quad (15)$$

Here, we introduced $t_e = t_{pd\sigma}^2/\Delta_e$, and

$$\alpha = 1 - \frac{D^2}{2\Delta\Delta_e} \left(\frac{\Delta + \Delta_e}{U} - 1 \right),$$

$$\frac{1}{\tilde{U}} = \frac{1}{2} \left(\frac{1}{U+D} + \frac{1}{U-D} \right). \quad (16)$$

In these equations, $\Delta_e = \Delta + D$ stands for $p \rightarrow e_g$ charge-transfer energy, see Fig. 4(a). Parameter D represents a difference between the pd charge-transfer gaps for t_{2g} and e_g states; we note that it is actually smaller than a single-electron cubic splitting $10Dq$ due to excitonic effects. Namely, pd excitation energy Δ_{pd} is renormalized by electron-hole attraction: $\Delta_{pd} \rightarrow (E_d - E_p) - U_{pd}$. Due to different spatial shapes of the orbitals, involved in π - and σ -type bondings [see Fig. 4(b)], one has $U_{pd\sigma} > U_{pd\pi}$. As a result,

$$D = 10Dq - \delta U_{pd}, \quad \text{with } \delta U_{pd} = U_{pd\sigma} - U_{pd\pi}. \quad (17)$$

The exchange Hamiltonian (15), projected onto pseudospin-1/2 sector reads as:

$$\mathcal{H}_{\text{BI}}^{(c)} = \frac{80\alpha}{81} \frac{tt_e}{\tilde{U}} \left(\tilde{\mathbf{S}}_i \cdot \tilde{\mathbf{S}}_j - \frac{1}{2} \tilde{S}_i^z \tilde{S}_j^z \right), \quad (18)$$

comprising AF Heisenberg and FM Kitaev terms.

2. Charge-transfer processes

There are two distinct charge-transfer contributions involving t_{2g} and e_g orbitals, see Figs. 8(b) and (c). Calculations similar to those in subsection-A2 above result in the spin-orbital Hamiltonian:

$$\mathcal{H}_{\text{B2}}^{(c)} = \frac{8\beta}{9} \frac{tt_e}{\Delta + \frac{U_p}{2}} (\mathbf{S}_i \cdot \mathbf{S}_j - S^2)(n_{ic} + n_{jc})$$

$$- \frac{2\gamma}{9} \frac{tt_e J_H^p}{(\Delta + \frac{D+U_p'}{2})^2} \mathbf{S}_i \cdot \mathbf{S}_j (n_{ab}^i + n_{ab}^j). \quad (19)$$

Here, $n_{ab} = n_a + n_b$, and parameters

$$\beta = 1 - \frac{D}{4(\Delta_e + \frac{U_p}{2})} + \frac{D U_p}{8\Delta(\Delta_e + \frac{U_p}{2})} - \frac{D}{4\Delta_e},$$

$$\gamma = \frac{(\Delta + \Delta_e)^2}{4\Delta\Delta_e}. \quad (20)$$

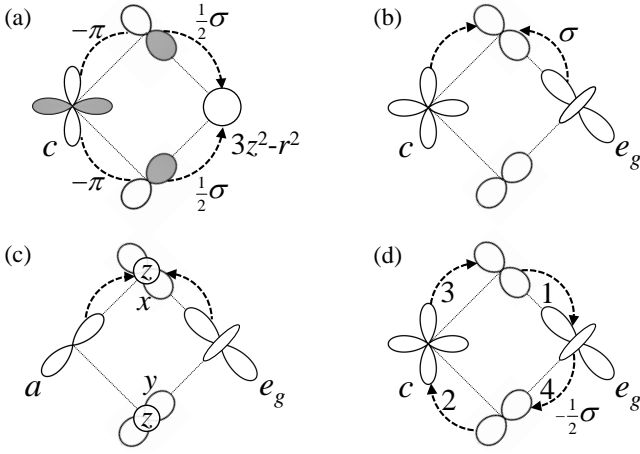


FIG. 8. Schematic of $t_{2g} - e_g$ hopping processes. π (σ) represents the $t_{pd\pi}$ ($t_{pd\sigma}$) overlap between t_{2g} (e_g) and p orbitals. (a) Intersite U process resulting from hopping of $c = d_{xy}$ orbital to $e_g(3z^2 - r^2)$ orbital. In this panel, the shaded (blank) lobes of wavefunctions imply a positive (negative) sign. (b), (c) Charge-transfer processes when two holes meet each other at an oxygen ion, and occupy either (b) the same p orbital, or (c) different p orbitals and interact via Hund's coupling J_H^p . (d) An example of the cyclic exchange process. The numbers 1,2,3,4 indicate the time order of the pd -hoppings of electrons. The overlap between e_g orbital and lower oxygen p_y orbital obtains a prefactor $(-1/2)$.

After projecting Eq. (19) onto the Kramers doublet, one obtains the pseudospin-1/2 exchange Hamiltonian:

$$\mathcal{H}_{B2}^{(c)} = \frac{20\beta}{27} \frac{8}{3} \frac{tt_e}{\Delta + \frac{U_p}{2}} \left(\tilde{\mathbf{S}}_i \cdot \tilde{\mathbf{S}}_j - \frac{1}{2} \tilde{S}_i^z \tilde{S}_j^z \right) - \frac{20\gamma}{27} \frac{tt_e J_H^p}{(\Delta + \frac{D+U'_p}{2})^2} \left(\tilde{\mathbf{S}}_i \cdot \tilde{\mathbf{S}}_j + \frac{1}{3} \tilde{S}_i^z \tilde{S}_j^z \right). \quad (21)$$

3. Cyclic exchange processes

This process involves c and e_g orbitals as depicted in Fig. 8(d). As discussed in subsection-A3, the cyclic exchange Hamiltonian can be expressed via Dirac spin permutation operator, and orbital projector n_c (for a c bond):

$$\mathcal{H}_{B3}^{(c)} = -\frac{2\zeta}{9} \frac{tt_e}{\Delta} (\mathbf{S}_i \cdot \mathbf{S}_j + S^2)(n_{ic} + n_{ic}), \quad (22)$$

with

$$\zeta = 1 - \frac{1}{2} \frac{D}{\Delta + D}. \quad (23)$$

As compared to $t_{2g} - t_{2g}$ cyclic exchange (11), an overall negative sign appears in Eq. (22); it originates from $p_y - e_g$ overlap phase factor $(-1/2)$ indicated in Fig. 8(d).

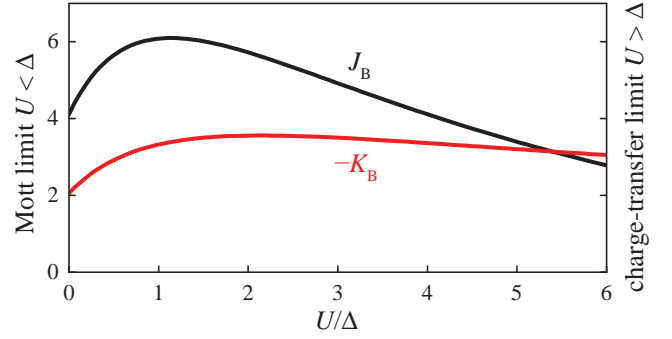


FIG. 9. $t_{2g} - e_g$ contribution to Heisenberg (J_B) and Kitaev ($-K_B$) couplings in units of t^2/U as a function of U/Δ . The parameters used are: $J_H^p/U_p = 0.3$ [35], $t_{pd\sigma}/t_{pd\pi} = 2$, $D/U = 0.2$, and $U_p/U = 0.7$.

The corresponding pseudospin-1/2 exchange Hamiltonian is:

$$\mathcal{H}_{B3}^{(c)} = -\frac{40\zeta}{81} \frac{tt_e}{\Delta} \left(\tilde{\mathbf{S}}_i \cdot \tilde{\mathbf{S}}_j - \frac{1}{2} \tilde{S}_i^z \tilde{S}_j^z \right). \quad (24)$$

Putting now together all the three $t_{2g} - e_g$ contributions above, $\mathcal{H}_{B1}^{(c)} + \mathcal{H}_{B2}^{(c)} + \mathcal{H}_{B3}^{(c)}$, we get:

$$\mathcal{H}_B^{(c)} = J_B \tilde{\mathbf{S}}_i \cdot \tilde{\mathbf{S}}_j + K_B \tilde{S}_i^z \tilde{S}_j^z, \quad (25)$$

with

$$J_B = +\frac{80}{81} tt_e \left[\frac{\alpha}{\tilde{U}} + \frac{2\beta}{\Delta + \frac{U_p}{2}} - \frac{3\gamma}{4} \frac{J_H^p}{(\Delta + \frac{D+U'_p}{2})^2} - \frac{\zeta}{2\Delta} \right],$$

$$K_B = -\frac{40}{81} tt_e \left[\frac{\alpha}{\tilde{U}} + \frac{2\beta}{\Delta + \frac{U_p}{2}} + \frac{\gamma}{2} \frac{J_H^p}{(\Delta + \frac{D+U'_p}{2})^2} - \frac{\zeta}{2\Delta} \right]. \quad (26)$$

In Fig. 9, we show how Heisenberg (J_B) and Kitaev ($-K_B$) couplings vary as a function of U/Δ . As in the case of $t_{2g} - t_{2g}$ exchange, J_B dominates in Mott limit. When U/Δ increases, the charge-transfer and cyclic exchange contributions gradually increase, resulting in comparable values of FM Kitaev and AF Heisenberg couplings.

Comparing the overall values of $t_{2g} - t_{2g}$ and $t_{2g} - e_g$ exchange contributions, represented in Figs. 7 and 9 correspondingly, one immediately notices the dominance of the $t_{2g} - e_g$ exchange channel, as expected on general grounds: as noticed above, $t_{2g} - e_g$ hopping is the largest one in 90° bonding geometry [9, 36], and the d^7 pseudospin-1/2 wavefunction contains a large weight of the e_g -level spin density.

C. $e_g - e_g$ exchange processes

Finally, we consider the pseudospin interactions originating from nearest-neighbor coupling of the spins re-

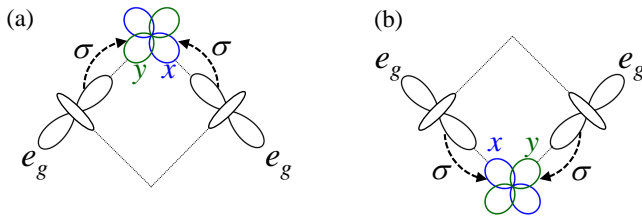


FIG. 10. Schematic of the $e_g - e_g$ charge-transfer exchange process leading to ferromagnetic Heisenberg coupling. Two holes meet on (a) upper oxygen or (b) lower oxygen ions, and interact via Hund's coupling J_H^p . σ stands for $t_{pd\sigma}$ hopping between e_g orbitals and p_x (blue) and p_y (green) orbitals.

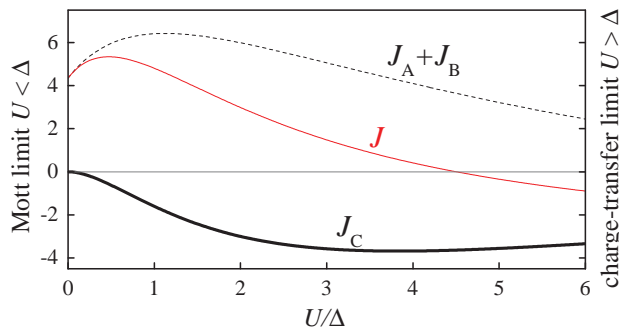


FIG. 11. Ferromagnetic (of negative sign) Heisenberg coupling J_C from $e_g - e_g$ hopping process, in units of t^2/U , as a function of U/Δ . In a charge-transfer regime of large U/Δ , J_C nearly compensates antiferromagnetic $J_A + J_B$ contribution (dashed line) from $t_{2g} - t_{2g}$ and $t_{2g} - e_g$ hoppings, resulting in strong suppression and sign-change of overall Heisenberg coupling J (red thin line). The parameters used are: $J_H^p/U_p=0.3$ [35], $t_{pd\pi}/t_{pd\sigma} = 2$, $D/U = 0.2$, and $U_p/U = 0.7$.

siding on e_g orbitals, see Fig. 2(c). In 90° bonding geometry, both U and cyclic-exchange processes of e_g spins vanish by symmetry, and we are left with the charge-transfer process alone, where two holes are transferred to an oxygen ion and interact via Hund's coupling J_H^p , see Fig. 10. Similar to the $t_{2g} - t_{2g}$ charge-transfer process in Fig. 6(b), this contribution gives FM coupling, as expected from Goodenough-Kanamori rules [37] for orbitals that do not directly overlap and interact via Hund's coupling.

After calculations following subsection-A2 above, we find the $e_g - e_g$ charge-transfer contribution to the exchange Hamiltonian:

$$\mathcal{H}_C^{(c)} = -\frac{4}{9} \frac{t_e^2 J_H^p}{(\Delta_e + \frac{U'_p}{2})^2} \mathbf{S}_i \cdot \mathbf{S}_j. \quad (27)$$

This is a pure-spin interaction, since both e_g orbitals are half-filled (no e_g orbital degeneracy). Consequently, after projecting onto pseudospin subspace, the interaction

preserves its SU(2) invariant Heisenberg form:

$$\mathcal{H}_C^{(c)} = J_C \tilde{\mathbf{S}}_i \cdot \tilde{\mathbf{S}}_j, \quad (28)$$

with

$$J_C = -\frac{100}{81} \frac{t_e^2 J_H^p}{(\Delta_e + \frac{U'_p}{2})^2}. \quad (29)$$

In Fig. 11, we plot J_C as a function of U/Δ , using the same representative parameters as in Figs. 7 and 9 above. For comparison, we show also Heisenberg AF coupling $J_A + J_B$ originating from $t_{2g} - t_{2g}$ and $t_{2g} - e_g$ channels, as well as total value of J . It follows that the FM exchange coupling J_C largely compensates the AF contributions of other channels, as one goes from Mott limit to charge-transfer regime of large U/Δ .

IV. OVERALL VALUES OF J AND K: INTERPLAY BETWEEN DIFFERENT EXCHANGE MECHANISMS

Having quantified the basic exchange channels for d^7 ions, we are now in position to put the results together:

$$\mathcal{H}_{ij}^{(c)} = J \tilde{\mathbf{S}}_i \cdot \tilde{\mathbf{S}}_j + K \tilde{S}_i^z \tilde{S}_j^z + \Gamma (\tilde{S}_i^x \tilde{S}_j^y + \tilde{S}_i^y \tilde{S}_j^x), \quad (30)$$

with coupling constants

$$\begin{aligned} J &= J_A + J_B + J_C, \\ K &= K_A + K_B, \\ \Gamma &= \Gamma_A. \end{aligned} \quad (31)$$

The explicit expressions for individual A($t_{2g} - t_{2g}$), B($t_{2g} - e_g$), and C($e_g - e_g$) contributions to the exchange constants are given by Eqs. (14), (26), and (29), respectively. Using these equations, which constitute the main results of the present work, one can readily evaluate the overall values of the Hamiltonian parameters J , K , and Γ , and obtain their dependence on material specific parameters such as Δ , D , J_H^p , etc.

As an example, we show in Figs. 12(a) and 12(b) the Heisenberg and Kitaev-type couplings as a function of U/Δ , calculated for two different values of parameter D . We recall that D is "an effective $10Dq$ " value in the context of charge-transfer physics, that is a difference between $p \rightarrow e_g$ and $p \rightarrow t_{2g}$ charge-transfer gaps, renormalized by excitonic effects, see Eq. (17). In both panels, the Kitaev coupling is always negative and its value tends to gradually increase with U/Δ . Most important observation is that Heisenberg coupling J is strongly suppressed and changes its sign in the charge-transfer regime of large U/Δ , due to enhanced FM coupling between e_g spins as found above. The resulting spin-liquid window with $|J| \ll -K$ shifts towards lower values of U/Δ , when a difference D between t_{2g} and e_g charge-transfer gaps decreases. Physically, this parameter depends on material properties such as degree of covalency, crystal structure,

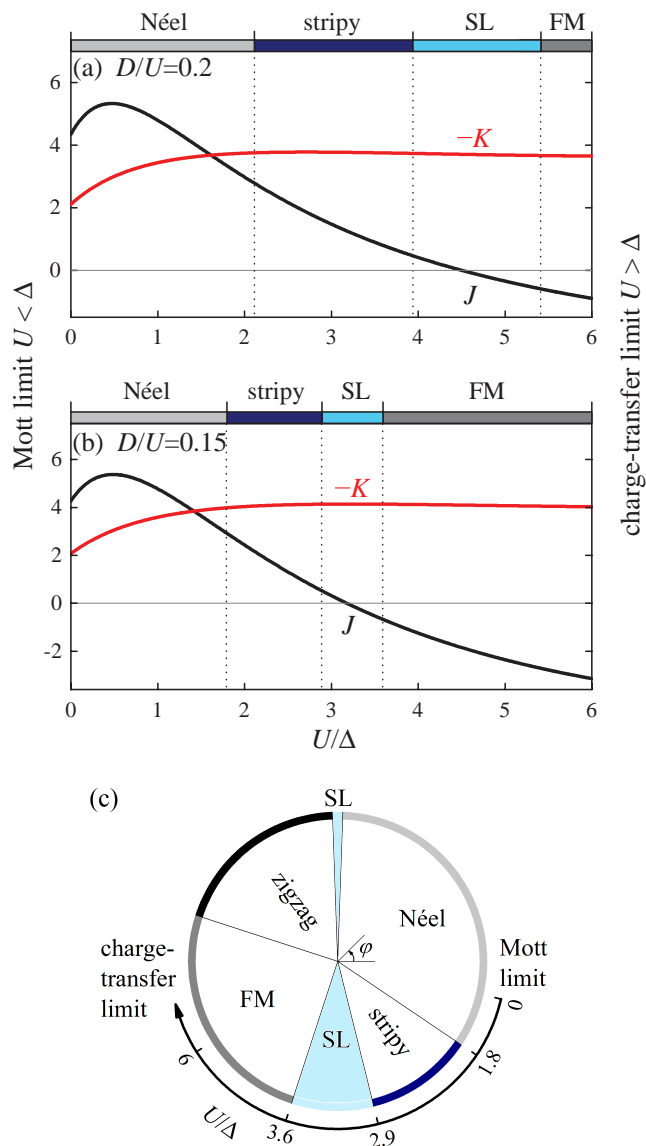


FIG. 12. Total values of Heisenberg (J) and Kitaev ($-K$) couplings in units of t^2/U as a function of U/Δ , calculated with (a) $D/U=0.2$ and (b) $D/U=0.15$. Other parameters used are: $J_H^p/U_p=0.3$ [35], $t_{pd\pi}/t_{pd\sigma} = 2$, $U_p/U = 0.7$, and $\kappa = 0.2$. Phase boundaries are obtained using the results of Refs. 12 and 34. (c) Projection of the phase boundaries shown in panel (b) onto the phase diagram of the Kitaev-Heisenberg model in the φ -angle representation of Eq. (32).

etc. For example, from the optical absorption data in CoO [27], we infer $D \sim 1$ eV; with the ab initio estimates $U \sim 5.0 - 7.8$ eV [38–40] this gives $D/U \sim 0.13 - 0.20$.

Regarding U/Δ parameter in cobalt compounds, this may vary broadly depending on material chemistry, in particular on the electronegativity of the anions. While $\Delta \sim 4$ eV in oxides, this value is much reduced in compounds with Cl, S, P, etc. [22, 41], so that $\Delta \sim 2 - 4$ eV and $U/\Delta \sim 2 - 3$ values seem to be plausible in cobalt

compounds. Given that the Hund’s coupling effects shift the Kitaev spin-liquid window towards much lower values of $U/\Delta \sim 1 - 3$ in the phase diagram (see Appendix), the charge-transfer type cobalt insulators may indeed realize the Kitaev-type interactions that dominate over isotropic Heisenberg couplings.

The Γ -coupling in Eq. (30) is contributed by $t_{2g} - t_{2g}$ process (14) only, and small when a direct hopping t' is weak as compared to oxygen-mediated t hopping. The phase diagram of $J - K$ model alone is often presented in literature using the following φ -angle parametrization [34]:

$$\mathcal{H}_{ij}^{(c)} = A(2 \sin\varphi \tilde{S}_i^z \tilde{S}_j^z + \cos\varphi \tilde{\mathbf{S}}_i \cdot \tilde{\mathbf{S}}_j). \quad (32)$$

The energy scale A and angle φ are given by $J = A \cos\varphi$ and $K = 2A \sin\varphi$. For completeness, we use this parametrization and map the results of Fig. 12(b) onto the φ -angle phase diagram, see Fig. 12(c). This figure quantifies the phase behavior of d^7 pseudospin-1/2 system as a function of U/Δ , evolving from Néel AF in Mott limit to FM state in charge-transfer regime, through an intermediate Kitaev spin-liquid phase.

Recently, new cobalt compounds $\text{Na}_2\text{Co}_2\text{TeO}_6$ and $\text{Na}_3\text{Co}_2\text{SbO}_6$ with a nearly perfect honeycomb lattice of magnetic Co^{2+} d^7 ions have been synthesized and studied [23–26]. Both these two systems develop a zigzag-type antiferromagnetic order at low temperatures, analogous to that observed in d^5 pseudospin-1/2 materials RuCl_3 and Na_2IrO_3 . The zigzag-AF order can be stabilized within the Kitaev-Heisenberg model with $K > 0$ [34], or with the help of longer-range Heisenberg couplings [42, 43] if $K < 0$. Since we found above that the sign of Kitaev coupling in d^7 pseudospin-1/2 cobaltates is robustly negative for any values of U/Δ , it seems that the zigzag-type AF in $\text{Na}_2\text{Co}_2\text{TeO}_6$ and $\text{Na}_3\text{Co}_2\text{SbO}_6$ is supported by $K < 0$ and long-range J couplings. As a side remark, we notice that the long-range pseudospin interactions are expected to be predominantly isotropic, since many exchange paths are involved and thus bond-directional nature of orbitals (leading to Kitaev-type interactions at short, nearest-neighbor distances) can be effectively averaged out at long distances.

In this work, we assumed an ideal cubic symmetry of the pseudospin-1/2 wave functions. Trigonal distortions, likely to be present in real materials, can induce additional anisotropic terms in the Hamiltonian and affect the phase boundaries. Neutron and resonant x-ray scattering measurements similar to those done in RuCl_3 and Na_2IrO_3 (see, e.g., Refs. 43–45) are necessary to quantify the exchange parameters in d^7 pseudospin-1/2 cobalt compounds. Useful information on anisotropic exchange terms can be deduced also from the analysis of magnetic anisotropy [46–48] and magnetization [49] data.

V. CONCLUSIONS

In this paper, we have presented a comprehensive study of the spin-orbital exchange interactions between d^7 ions with $t_{2g}^5 e_g^2$ electronic configuration. Various exchange channels, involving t_{2g} and e_g orbital interactions in 90° bonding geometry, have been examined in detail and quantified. The exchange processes considered here are generic to many transition metal compounds, in particular when both t_{2g} and e_g orbitals are spin active.

In a cubic crystal field, the d^7 ions with $S = 3/2$ and effective orbital momentum $L = 1$ form a pseudospin-1/2 ground state. We have projected spin-orbital interactions onto this doublet, and obtained the Kitaev-Heisenberg model as a low-energy magnetic Hamiltonian, with the dominant K term in case of charge-transfer insulating regime. This is in contrast to d^7 cobaltates with 180° bonding geometry such as KCoF_3 , where isotropic Heisenberg coupling J dominates pseudospin-1/2 interactions [16, 17], just as in d^5 pseudospin-1/2 perovskite Sr_2IrO_4 [30].

In d^5 compounds such as Na_xCoO_2 , RuCl_3 , and Na_2IrO_3 , a suppression of Heisenberg J coupling is due to cancellation of the $t_{2g} - t_{2g}$ channel U processes in 90° bonding exchange geometry [9, 11]. In d^7 cobaltates, we found instead that a suppression of J coupling is due to ferromagnetic spin exchange of e_g electrons, which may largely compensate the AF contribution of other channels or even change the sign of J . This mechanism of J -suppression in favor of Kitaev term requires a closeness to charge-transfer insulating regime. Since cobalt oxides typically belong to this category of insulators [22], zigzag-AF order observed in honeycomb lattice cobaltates $\text{Na}_2\text{Co}_2\text{TeO}_6$ and $\text{Na}_3\text{Co}_2\text{SbO}_6$ is likely to have the same origin as in RuCl_3 and Na_2IrO_3 , that is, due to FM Kitaev-type interactions combined with long-range J couplings.

Apart from honeycomb lattice compounds [23–26, 41, 50, 51], there are many d^7 cobaltates possessing pseudospin-1/2 ground state, such as quasi-one dimensional CoNb_2O_6 [52], triangular lattice antiferromagnets $\text{Ba}_3\text{CoSb}_2\text{O}_9$ [53] and $\text{Ba}_8\text{CoNb}_6\text{O}_{24}$ [54], spinel GeCo_2O_4 [28] and pyrochlore lattice $\text{NaCaCo}_2\text{F}_7$ [29, 55] cobaltates. Even though the bonding geometries are no longer exactly 90° , a strongly anisotropic, bond-dependent Ising interactions as in d^5 (or in f -electron [56]) systems are expected in these materials.

Altogether, the results presented in this work suggest that cobalt based compounds are of interest in the context of pseudospin-1/2 magnetism in general, and Kitaev model physics in particular, and, as such, they deserve more focused experimental studies.

Note added. Recently, we became aware that a similar idea has been proposed independently by Sano *et al.* [57].

ACKNOWLEDGMENTS

We would like to thank J. Chaloupka for useful discussions. We acknowledge support by the European Research Council under Advanced Grant No. 669550 (Com4Com).

Appendix A: Hund's coupling effects

The energies and wavefunctions of the intermediate states, created during the exchange processes, are affected by intraionic Hund's coupling. This leads to corrections of the order of J_H/U to the exchange Hamiltonians (see, e.g., Ref. [9]). Below, we consider the Hund's coupling effects on d^7 pseudospin-1/2 interactions, and show that they tend to suppress AF coupling J and hence further support the Kitaev spin-liquid regime.

A minimal model for the on-site Coulomb and exchange interactions can be cast in the following form:

$$\begin{aligned} \mathcal{H}_{\text{loc}} = & U \sum_{i,\alpha} n_{i\alpha\uparrow} n_{i\alpha\downarrow} + \sum_{i,\alpha < \beta} \left(U' - J_H \hat{P}_s \right) n_{i\alpha} n_{i\beta} \\ & + J_H \sum_{i,\alpha \neq \beta} d_{\alpha\uparrow}^\dagger d_{\alpha\downarrow}^\dagger d_{\beta\downarrow} d_{\beta\uparrow}. \end{aligned} \quad (\text{A1})$$

Here, $\hat{P}_s = (2\mathbf{s}_{i\alpha}\mathbf{s}_{i\beta} + \frac{1}{2})$ is spin permutation operator, n_α and \mathbf{s}_α are the density and spin-1/2 operators on α -orbital, correspondingly. The last, so-called ‘‘pair-hopping’’ term describes a motion of doubly occupied orbital states. U and $U' = U - 2J_H$ stand for intraorbital and interorbital Coulomb repulsions, correspondingly (the spherical symmetry assumed), and $J_H = 3B + C \simeq 8B$ is Hund's coupling expressed in terms of Racah parameters B and C . The ratio J_H/U is subject to various screening effects and thus material sensitive. The representative values of $J_H \simeq 0.8$ eV (from optical data in CoO [27]) and $U \sim 5.0 - 7.8$ eV [38–40] seem to suggest the range of $0.1 < J_H/U < 0.2$, roughly.

Two different valence states of Co ion, d^6 and d^8 , can appear in the intermediate states. Fortunately, d^8 states $t_{2g}^6 e_g^2$ and $t_{2g}^5 e_g^3$ are created by hopping processes always in the unique $S = 1$ state. Thus, we need to consider Hund's splitting of the d^6 intermediate states which appear in the Mott-Hubbard-type U processes $d_i^7 d_j^7 \rightarrow d_i^6 d_j^8$ only. The transition energies $E = E(d_i^6 d_j^8) - E(d_i^7 d_j^7)$ and matrix elements depend on the spin-orbital structure of the initial and intermediate states and hence on Hund's coupling.

1. t_{2g} - t_{2g} exchange

The t -hopping generates d^6 configuration either in the high-spin $S = 2$ state with corresponding excitation energy $E_1 = U - 3J_H$, or in the low-spin $S = 1$ states at energies $E_2 = U + J_H$ and $E_3 = U + 4J_H$. (We note that

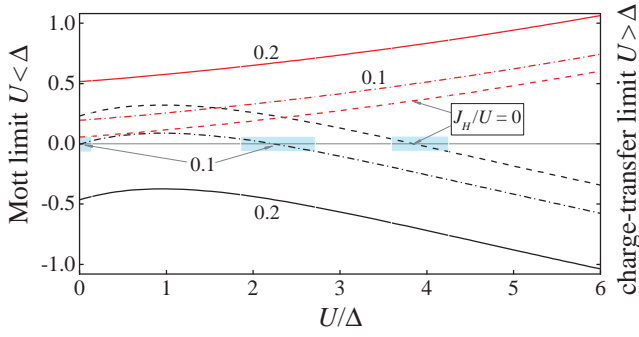


FIG. 13. t_{2g} - t_{2g} contribution to Heisenberg J_A (black lines) and Kitaev $-K_A$ (red lines) couplings in units of t^2/U as a function of U/Δ , calculated for different values of Hund's coupling: $J_H/U = 0$ (dashed), $J_H/U = 0.1$ (dash-dotted), and $J_H/U = 0.2$ (solid lines). The other parameters (and hence $J_H = 0$ results) are the same as in Fig. 7. Spin-liquid windows (colored rectangles) are obtained using the results of Refs. 12 and 34.

pair-hopping term is essential for obtaining the $S = 1$ state energies and wave functions).

For simplicity, we neglect J_H/U corrections to small t' hopping processes (as in the main text, we will show the results for $\kappa = t'/t = 0.2$), and focus on oxygen-mediated t hoppings. After somewhat tedious but straightforward calculations, the exchange contribution $\mathcal{H}_{A1}^{(c)}$ from t_{2g} - t_{2g} hoppings $\propto t^2/U$ is obtained as follows:

$$\begin{aligned}
& \frac{4t^2}{9} \frac{1}{E_1} (\mathbf{S}_i \cdot \mathbf{S}_j + S^2) (a_i^\dagger b_i a_j^\dagger b_j + b_i^\dagger a_i b_j^\dagger a_j) \\
& + \frac{4t^2}{27} \left(\frac{1}{E_3} + \frac{2}{E_2} \right) (\mathbf{S}_i \cdot \mathbf{S}_j + S^2) (n_{ia} n_{jb} + n_{ib} n_{ja}) \\
& - \frac{t^2}{6} \left(\frac{1}{E_1} - \frac{1}{E_2} \right) (\mathbf{S}_i \cdot \mathbf{S}_j + S^2) [(n_{ia} - n_{jb})^2 + (n_{ib} - n_{ja})^2] \\
& - \frac{4t^2}{27} \left(\frac{1}{E_2} - \frac{1}{E_3} \right) (\mathbf{S}_i \cdot \mathbf{S}_j - S^2) (a_i^\dagger b_i b_j^\dagger a_j + b_i^\dagger a_i a_j^\dagger b_j) \\
& + \frac{t^2}{6} \left(\frac{3}{E_1} + \frac{1}{E_2} - \frac{4}{E_3} \right) (n_{ia} n_{jb} + n_{ib} n_{ja}). \quad (\text{A2})
\end{aligned}$$

When $J_H = 0$, i.e. $E_n = U$, Eq. A2 fully recovers the first line ($\propto \frac{t^2}{U}$ term) of Eq. 3.

After projection onto pseudospin-1/2 doublet, this Hamiltonian reads as

$$\mathcal{H}_{A1}^{(c)} = J_{A1}^{(c)} \tilde{\mathbf{S}}_i \cdot \tilde{\mathbf{S}}_j + K_{A1}^{(c)} \tilde{S}_i^z \tilde{S}_j^z, \quad (\text{A3})$$

with the exchange parameters:

$$\begin{aligned}
J_{A1}^{(c)} &= + \frac{t^2}{81} \left(-\frac{31}{E_1} + \frac{43}{E_2} + \frac{6}{E_3} \right), \\
K_{A1}^{(c)} &= - \frac{t^2}{81} \left(\frac{23}{E_1} - \frac{61}{3E_2} + \frac{4}{3E_3} \right). \quad (\text{A4})
\end{aligned}$$

In the limit of $J_H = 0$ (set $E_n = U$), this gives $J_{A1}^{(c)} = \frac{2}{9} \frac{t^2}{U}$

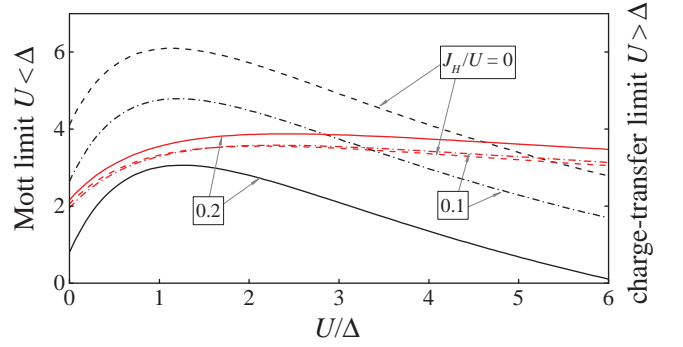


FIG. 14. t_{2g} - e_g contribution to Heisenberg J_B (black lines) and Kitaev $-K_B$ (red lines) couplings in units of t^2/U as a function of U/Δ , calculated for different values of Hund's coupling: $J_H/U = 0$ (dashed), $J_H/U = 0.1$ (dash-dotted), and $J_H/U = 0.2$ (solid lines). The other parameters (and hence $J_H = 0$ results) are the same as in Fig. 9.

and $K_{A1}^{(c)} = -\frac{4}{81} \frac{t^2}{U}$, reproducing the results $\propto t^2/U$ of the main text (see first line of Eq. 7).

We now replace the first terms ($\propto t^2/U$) of J_A and K_A in Eq. 14 by the corresponding results from Eq. A4 (the charge-transfer and cyclic exchange terms $\propto t^2/\Delta$ are not affected by Hund's coupling). The results presented in Fig. 13 show that Hund's coupling corrections suppress the AF J interaction, which eventually becomes FM for all U/Δ values when J_H/U is large enough. For the intermediate values of $J_H/U \sim 0.1$, the spin-liquid window appears around $U/\Delta \sim 2$ as well as in the Mott limit.

At this point, we recall that the t_{2g} - t_{2g} contribution is in fact much weaker than the t_{2g} - e_g exchange terms in d^7 systems. Therefore, Hund's coupling affects J and K parameters predominantly via the latter channel, as shown below.

2. t_{2g} - e_g exchange

The t_{2g} - e_g hoppings generate d^6 intermediate states with both high $S = 2$ and low $S = 1$ spins, too, but the energies $E_{1,2,3}$ defined above are now shifted by splitting D between t_{2g} and e_g orbitals. Collecting all possible transitions with the corresponding matrix elements, we find that at finite Hund's coupling the Hamiltonian $\mathcal{H}_{B1}^{(c)}$ in Eq. 15 takes the following form:

$$\begin{aligned}
\mathcal{H}_{B1}^{(c)} &= \frac{4\alpha}{9} \frac{tt_e}{\tilde{U}} (\mathbf{S}_i \cdot \mathbf{S}_j - S^2) (n_{ic} + n_{jc}) \\
& - \frac{tt_e}{6} \frac{\Delta_e}{\Delta} \left(\frac{1}{E_1 + D} - \frac{1}{E_2 + D} \right) \mathbf{S}_i \cdot \mathbf{S}_j (n_{ab}^i + n_{ab}^j), \quad (\text{A5})
\end{aligned}$$

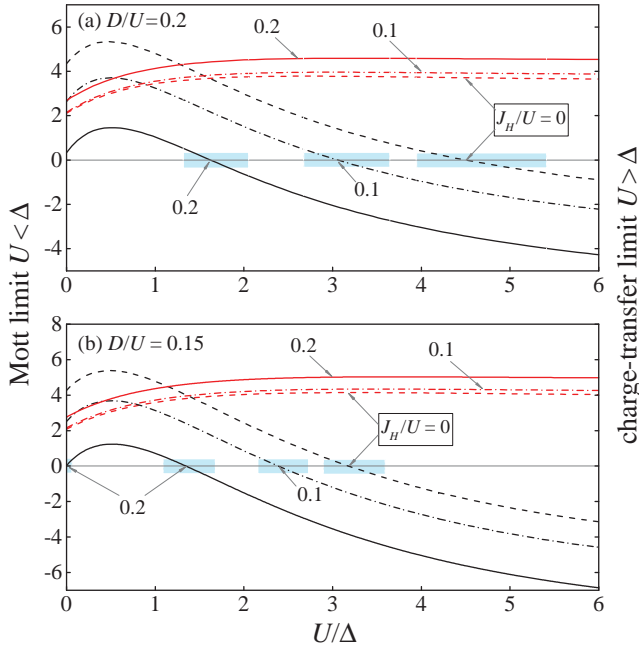


FIG. 15. Total values of Heisenberg J (black lines) and Kitaev $-K$ (red lines) couplings in units of t^2/U as a function of U/Δ , calculated with (a) $D/U=0.2$ and (b) $D/U=0.15$ at different Hund's couplings: $J_H/U = 0$ (dashed), $J_H/U = 0.1$ (dash-dotted), and $J_H/U = 0.2$ (solid lines). The other parameters (and hence $J_H = 0$ results) are the same as in Fig. 12. Spin-liquid windows (colored rectangles) are obtained using the results of Refs. 12 and 34. For $J_H/U = 0.2$, small spin-liquid phase appears also in the Mott limit of $U/\Delta = 0$.

with the renormalized constants α and $1/\tilde{U}$:

$$\alpha = 1 - \frac{D^2}{2\Delta\Delta_e} \left(\frac{\Delta + \Delta_e}{U + 2J_H} - 1 \right),$$

$$\frac{1}{\tilde{U}} = \frac{1}{6} \left(\frac{2}{E_2 + D} + \frac{1}{E_3 + D} + \frac{3}{U + 2J_H - D} \right). \quad (\text{A6})$$

We recall that $n_{ab} = n_a + n_b = 1 - n_c$ (in hole representation). Note also that new transition energy $U + 2J_H - D$ appeared in $1/\tilde{U}$. This corresponds to $d^6(t_{2g}^5 e_g^1)$ state

with two holes on an e_g orbital; its pair-hopping motion to the t_{2g} levels is suppressed by $2D > J_H$ splitting.

After projection onto pseudospin-1/2 doublet, the Hamiltonian reads as

$$\mathcal{H}_{\text{B1}}^{(c)} = J_{\text{B1}}^{(c)} \tilde{\mathbf{S}}_i \cdot \tilde{\mathbf{S}}_j + K_{\text{B1}}^{(c)} \tilde{S}_i^z \tilde{S}_j^z, \quad (\text{A7})$$

with exchange parameters:

$$J_{\text{B1}}^{(c)} = +\frac{80}{81} tt_e \left[\frac{\alpha}{\tilde{U}} - \frac{9\Delta_e}{16\Delta} \left(\frac{1}{E_1 + D} - \frac{1}{E_2 + D} \right) \right],$$

$$K_{\text{B1}}^{(c)} = -\frac{40}{81} tt_e \left[\frac{\alpha}{\tilde{U}} + \frac{3\Delta_e}{8\Delta} \left(\frac{1}{E_1 + D} - \frac{1}{E_2 + D} \right) \right]. \quad (\text{A8})$$

These equations tell that Hund's coupling tends to reduce AF J and increase FM K values [these corrections originate from the last term in Eq. A5]. When $J_H = 0$ (set $E_n = U$), these results recover Eq. 18 of the main text.

In Fig. 14, we show the t_{2g} - e_g hopping contribution to J_{B} and K_{B} values at different J_H/U ratios, including the $J_H = 0$ results of Fig. 9 for comparison. While K value remains nearly unaffected, Hund's coupling strongly suppresses AF J coupling, which, however, remains positive even at $J_H/U = 0.2$.

Having considered Hund's coupling effects both in the t_{2g} - t_{2g} and t_{2g} - e_g channels (e_g - e_g channel remains unchanged), we are ready to discuss the overall values of J and K parameters. Putting the results together into Eq. 31, we obtain the exchange parameters shown in Fig. 15 (including the $J_H = 0$ results of Fig. 12). As expected, the major effect of Hund's coupling is to shift down the J curves, such that Heisenberg coupling changes its sign at the lower values of U/Δ ratio. This implies that Hund's coupling cooperates with the charge-transfer effects to support Kitaev spin-liquid regime of $J/K \sim 0$. We observe that, at $J_H/U = 0.2$, this regime may appear also in the Mott limit, consistent with the recent work by Sano *et al.* [57].

Overall, it seems that Hund's coupling effects in d^7 pseudospin-1/2 compounds shift the spin-liquid parameter regime towards the lower values of U/Δ ratio, thereby increasing the chances of finding the Kitaev model physics in a broader class of d^7 cobalt compounds.

¹ A. Kitaev, Ann. Phys. (N.Y.) **321**, 2 (2006).

² M. Hermanns, I. Kimchi, and J. Knolle, Annu. Rev. Condens. Matter Phys. **9**, 17 (2018).

³ J. Knolle, *Dynamics of a Quantum Spin Liquid* (Springer, Berlin, 2016).

⁴ S. Trebst, arXiv:1701.07056 [cond-mat.str-el].

⁵ J. G. Rau, E. K.-H. Lee, and H.-Y. Kee, Annu. Rev. Condens. Matter Phys. **7**, 195 (2016).

⁶ S. M. Winter, A. A. Tsirlin, M. Daghofer, J. van den Brink, Y. Singh, P. Gegenwart, and R. Valentí, J. Phys.: Condens. Matter **29**, 493002 (2017).

⁷ K. I. Kugel and D. I. Khomskii, Sov. Phys. Usp. **25**, 231 (1982).

⁸ G. Khaliullin and S. Okamoto, Phys. Rev. B **68**, 205109 (2003); Phys. Rev. Lett. **89**, 167201 (2002).

⁹ G. Khaliullin, Prog. Theor. Phys. Suppl. **160**, 155 (2005).

¹⁰ G. Chen and L. Balents, Phys. Rev. B **78**, 094403 (2008).

¹¹ G. Jackeli and G. Khaliullin, Phys. Rev. Lett. **102**, 017205 (2009).

¹² J. Chaloupka, G. Jackeli, and G. Khaliullin, Phys. Rev. Lett. **105**, 027204 (2010).

¹³ G. Khaliullin, W. Koshibae, and S. Maekawa, Phys. Rev.

- Lett. **93**, 176401 (2004).
- ¹⁴ T. Hyart, A. R. Wright, G. Khaliullin, and B. Rosenow, Phys. Rev. B **85**, 140510(R) (2012).
 - ¹⁵ Y. Z. You, I. Kimchi, and A. Vishwanath, Phys. Rev. B **86**, 085145 (2012).
 - ¹⁶ T. M. Holden, W. J. L. Buyers, E. C. Svensson, R. A. Cowley, M. T. Hutchings, D. Hukin, and R. W. H. Stevenson, J. Phys. C: Solid State Phys. **4**, 2127 (1971).
 - ¹⁷ W. J. L. Buyers, T. M. Holden, E. C. Svensson, R. A. Cowley, and M. T. Hutchings, J. Phys. C: Solid State Phys. **4**, 2139 (1971).
 - ¹⁸ T. Yamada and O. Nakanishi, J. Phys. Soc. Jpn. **36**, 1304 (1974).
 - ¹⁹ J. P. Goff, D. A. Tennant, and S. E. Nagler, Phys. Rev. B **52**, 15992 (1995).
 - ²⁰ A. Abragam and B. Bleaney, *Electron Paramagnetic Resonance of Transition Ions* (Clarendon Press, Oxford, 1970).
 - ²¹ J. G. Rau, E. K.-H. Lee, and H.-Y. Kee, Phys. Rev. Lett. **112**, 077204 (2014).
 - ²² J. Zaanen, G. A. Sawatzky, and J. W. Allen, Phys. Rev. Lett. **55**, 418 (1985).
 - ²³ L. Viciu, Q. Huang, E. Morosan, H. W. Zandbergen, N. I. Greenbaum, T. McQueen, and R. J. Cava, J. Solid State Chem. **180**, 1060 (2007).
 - ²⁴ E. Lefrançois, M. Songvilay, J. Robert, G. Nataf, E. Jordan, L. Chaix, C. V. Colin, P. Lejay, A. Hadj-Azzem, R. Ballou, and V. Simonet, Phys. Rev. B **94**, 214416 (2016).
 - ²⁵ A. K. Bera, S. M. Yusuf, A. Kumar, and C. Ritter, Phys. Rev. B **95**, 094424 (2017).
 - ²⁶ C. Wong, M. Avdeev, and C. D. Ling, J. Solid State Chem. **243**, 18 (2016).
 - ²⁷ G. W. Pratt Jr. and R. Coelho, Phys. Rev. **116**, 281 (1959).
 - ²⁸ K. Tomiyasu, M. K. Crawford, D. T. Adroja, P. Manuel, A. Tominaga, S. Hara, H. Sato, T. Watanabe, S. I. Ikeda, J. W. Lynn, K. Iwasa, and K. Yamada, Phys. Rev. B **84**, 054405 (2011).
 - ²⁹ K. A. Ross, J. M. Brown, R. J. Cava, J. W. Krizan, S. E. Nagler, J. A. Rodriguez-Rivera, and M. B. Stone, Phys. Rev. B **95**, 144414 (2017).
 - ³⁰ J. Kim, D. Casa, M. H. Upton, T. Gog, Y.-J. Kim, J. F. Mitchell, M. van Veenendaal, M. Daghofer, J. van den Brink, G. Khaliullin, and B. J. Kim, Phys. Rev. Lett. **108**, 177003 (2012).
 - ³¹ Jungho Kim, M. Daghofer, A. H. Said, T. Gog, J. van den Brink, G. Khaliullin, and B. J. Kim, Nat. Commun. **5**, 4453 (2014).
 - ³² B. Normand and A. M. Oleś, Phys. Rev. B **78**, 094427 (2008).
 - ³³ J. Chaloupka and A. M. Oleś, Phys. Rev. B **83**, 094406 (2011).
 - ³⁴ J. Chaloupka, G. Jackeli, and G. Khaliullin, Phys. Rev. Lett. **110**, 097204 (2013).
 - ³⁵ K. Foyevtsova, H. O. Jeschke, I. I. Mazin, D. I. Khomskii, and R. Valentí, Phys. Rev. B **88**, 035107 (2013).
 - ³⁶ J. Chaloupka and G. Khaliullin, Prog. Theor. Phys. Suppl. **176**, 50 (2008).
 - ³⁷ J. B. Goodenough, *Magnetism and the Chemical Bond* (Interscience, New York, 1963).
 - ³⁸ V. I. Anisimov, J. Zaanen, and O. K. Andersen, Phys. Rev. B **44**, 943 (1991).
 - ³⁹ W. E. Pickett, S. C. Erwin, and E. C. Ethridge, Phys. Rev. B **58**, 1201 (1998).
 - ⁴⁰ H. Jiang, R. I. Gomez-Abal, P. Rinke, and M. Scheffler, Phys. Rev. B **82**, 045108 (2010).
 - ⁴¹ R. Brec, Solid State Ionics **22**, 3 (1986).
 - ⁴² I. Kimchi and Y.-Z. You, Phys. Rev. B **84**, 180407(R) (2011).
 - ⁴³ S. K. Choi, R. Coldea, A. N. Kolmogorov, T. Lancaster, I. I. Mazin, S. J. Blundell, P. G. Radaelli, Y. Singh, P. Gegenwart, K. R. Choi, S.-W. Cheong, P. J. Baker, C. Stock, and J. Taylor, Phys. Rev. Lett. **108**, 127204 (2012).
 - ⁴⁴ S. H. Chun, J.-W. Kim, Jungho Kim, H. Zheng, C. C. Stoumpos, C. D. Malliakas, J. F. Mitchell, K. Mehlawat, Y. Singh, Y. Choi, T. Gog, A. Al-Zein, M. Moretti Sala, M. Krisch, J. Chaloupka, G. Jackeli, G. Khaliullin, and B. J. Kim, Nature Phys. **11**, 462 (2015).
 - ⁴⁵ A. Banerjee, C. Bridges, J. Yan, A. Aczel, L. Li, M. Stone, G. Granroth, M. Lumsden, Y. Yiu, J. Knolle, D. Kovrizhin, S. Bhattacharjee, R. Moessner, D. Tennant, D. Mandrus, and S. E. Nagler, Nature Mater. **15**, 733 (2016).
 - ⁴⁶ J. Chaloupka and G. Khaliullin, Phys. Rev. B **92**, 024413 (2015).
 - ⁴⁷ J. Chaloupka and G. Khaliullin, Phys. Rev. B **94**, 064435 (2016).
 - ⁴⁸ Y. Sizyuk, P. Wölfle, and N. B. Perkins, Phys. Rev. B **94**, 085109 (2016).
 - ⁴⁹ L. Janssen, E. C. Andrade, and M. Vojta, Phys. Rev. B **96**, 064430 (2017).
 - ⁵⁰ R. David, H. Kabbour, A. Pautrat, and O. Mentré, Inorg. Chem. **52**, 8732 (2013).
 - ⁵¹ H. S. Nair, J. M. Brown, E. Coldren, G. Hester, M. P. Gelfand, A. Podlesnyak, Q. Huang, and K. A. Ross, arXiv:1712.06208 [cond-mat.str-el].
 - ⁵² R. Coldea, D. A. Tennant, E. M. Wheeler, E. Wawrzynska, D. Prabhakaran, M. Telling, K. Habicht, P. Smeibidl, and K. Kiefer, Science **327**, 177 (2010).
 - ⁵³ H. D. Zhou, C. Xu, A. M. Hallas, H. J. Silverstein, C. R. Wiebe, I. Umegaki, J. Q. Yan, T. P. Murphy, J.-H. Park, Y. Qiu, J. R. D. Copley, J. S. Gardner, and Y. Takano, Phys. Rev. Lett. **109**, 267206 (2012).
 - ⁵⁴ R. Rawl, L. Ge, H. Agrawal, Y. Kamiya, C. R. Dela Cruz, N. P. Butch, X. F. Sun, M. Lee, E. S. Choi, J. Oitmaa, C. D. Batista, M. Mourigal, H. D. Zhou, and J. Ma, Phys. Rev. B **95**, 060412(R) (2017).
 - ⁵⁵ K. A. Ross, J. W. Krizan, J. A. Rodriguez-Rivera, R. J. Cava, and C. L. Broholm, Phys. Rev. B **93**, 014433 (2016).
 - ⁵⁶ F. Y. Li, Y. D. Li, Y. Yu, A. Paramekanti, and G. Chen, Phys. Rev. B **95**, 085132 (2017).
 - ⁵⁷ R. Sano, Y. Kato, and Y. Motome, arXiv:1710.11357 [cond-mat.str-el].